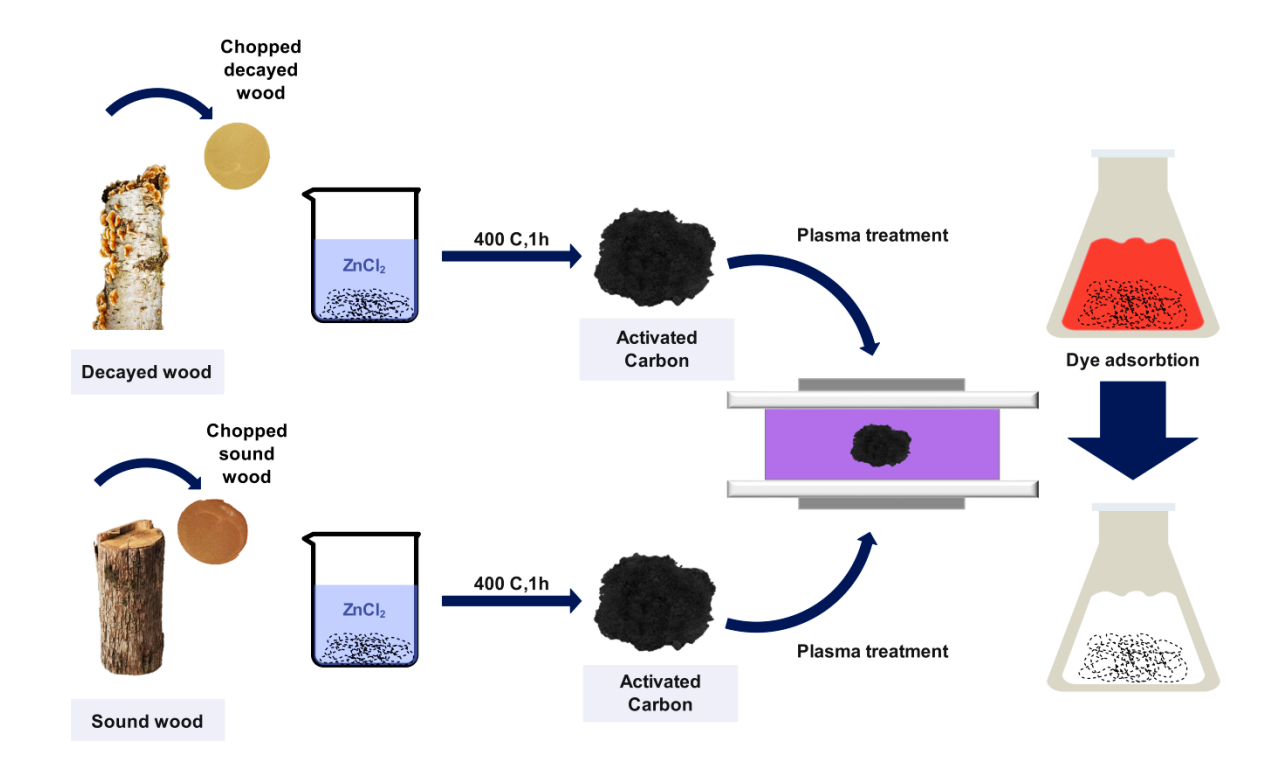
# Production of Activated Carbon from Decayed Wood: Surface Modification Using High-Frequency DBD Plasma for Enhanced Rhodamine B Dye Adsorption – A Kinetic and Equilibrium Study

Mahmood Roohbakhsh Bidaei,<sup>a</sup> Mohammad Azadfallah,<sup>a</sup> Rasoul Yarahmadi,<sup>b</sup> and Niloofar Goleij <sup>c,\*</sup>

\* Corresponding author: niloofar.goleij@modares.ac.ir

DOI: 10.15376/biores.19.4.9510-9530

## **GRAPHICAL ABSTRACT**



# Production of Activated Carbon from Decayed Wood: Surface Modification Using High-Frequency DBD Plasma for Enhanced Rhodamine B Dye Adsorption – A Kinetic and Equilibrium Study

Mahmood Roohbakhsh Bidaei, <sup>a</sup> Mohammad Azadfallah, <sup>a</sup> Rasoul Yarahmadi, <sup>b</sup> and Niloofar Goleij <sup>c,\*</sup>

The potential of decayed wood was investigated as a raw material to produce activated carbon. Both sound and decayed beech wood specimens were subjected to chemical activation with ZnCl<sub>2</sub> at a carbonization temperature of 400 °C and 75% impregnation ratio to produce activated carbon. The produced activated carbon was tested using Brunauer-Emmett-Teller, Fourier transform infrared, scanning electron microscopy, and thermogravimetric analyses to investigate its properties. The activated carbon was used to adsorb rhodamine B dye in an aqueous solution. Additionally, to investigate the impact of activated carbon surface modification on the adsorption of rhodamine B dye, both kinds of activated carbon underwent surface modification using dielectricbarrier discharge (DBD) plasma at a high frequency of 20 kHz in the air atmosphere for 20 min at a voltage level of 10 kV. The modification of the activated carbon substantially improved its characteristics, resulting in a 20% increase in rhodamine B removal for the activated carbon derived from sound wood and a 12% increase for the activated carbon derived from decayed wood. The utilization of DBD air plasma in this method is suitable because of its simplicity, cost-effectiveness, and improved adsorption capacity in activated carbon.

DOI: 10.15376/biores.19.4.9510-9530

Keywords: Decayed wood; Activated carbon; Plasma DBD; Rhodamine B; Dye adsorption

Contact information: a: Department of Wood and Paper Science and Technology, Faculty of Natural Resources, University of Tehran, Karaj, Iran; b: Air Pollution Research Center, Department of Occupational Health Engineering, Iran University of Medical Sciences, Tehran, Iran; c: Department of Occupational Health and Safety, Faculty of Medical Science, Tarbiat Modares University, Tehran, Iran \* Corresponding author: niloofar.goleij@modares.ac.ir

#### **Abbreviations**

AC Activated carbon

ACS Activated carbon from sound wood ACR Activated carbon from decayed wood

ACS-plasma Activated carbon from sound wood modified with plasma ACR-plasma Activated carbon from decayed wood modified with plasma

BET Brunauer–Emmett–Teller
C<sub>0</sub> Initial concentration (mg/L)
Ce Equilibrium concentration (mg/L)

Davg Mean pore diameter
DBD Dielectric-barrier discharge
FTIR Fourier-transform infrared

PPM Parts per million

RPM Revolutions per minute
SBET Specific surface area (m²/g)
Smi Micropore surface area
Vmi Micropore volume

VT Total pore volume (cm<sup>3</sup>/g)

#### INTRODUCTION

Lignocellulosic biomass is one of the most abundant renewable raw materials on Earth. It has an annual global photosynthetic production of approximately 182 billion tons, of which only about 8 billion tons are currently utilized (Blasi *et al.* 2023). These materials have great potential for conversion into useful products that promote the development of a circular and sustainable bioeconomy (Periyasamy *et al.* 2022).

There is a significant amount of decayed wood in forests that is either unused or used for burning in forest areas. Fungi are the primary agents in wood decomposition that cause the elimination of structural components of wood, such as lignin or cellulose, and also decrease the weight and mechanical and physical strength of wood (Karim *et al.* 2016). Annual wood rot results in the devastation of trees and wooden edifices, incurring millions of dollars in losses. The growth of fungi not only leads to the decay of standing trees but also diminishes wood strength (Schwarze 2007). Muller and Bütler (2010), reported the amount of decayed wood in European forests ranges from 10 to 150 cubic meters per hectare. Considering the capacity of decayed wood in forest areas and its lack of use in urban structures and industries, such as papermaking and wood composite production, this wood may hold significant potential for producing activated carbon.

In the adsorption process, activated carbon is one of the most important and unique adsorbents. There are four forms of activated carbon: granules, powder, plates, and fibers, each having specific applications. Activated carbon fibers typically find application in the recovery of organic solvents, CO<sub>2</sub> adsorption masks, the removal of volatile organic compounds, wastewater treatment, and energy applications (Hassan *et al.* 2020). Activated carbon granules are commonly employed in aqueous solutions and adsorption columns for water purification (Jjagwe *et al.* 2021), air purification (Wee *et al.* 2022), and the extraction of precious metals (Mpinga *et al.* 2014). Powdered activated carbon, derived from sawdust through a chemical activation process, is utilized in air filters to remove nitrogen pollutants and sulfur from the air (Sung *et al.* 2019). Unlike granules, which are physically produced from coal, powdered activated carbons exhibit lower diffusion resistance to adsorption. Extruded activated carbons, produced by combining carbonaceous raw materials with binding agents such as wood, bituminous materials, resins, and petroleum by-products, serve similar applications to granular activated carbons (Świątkowski 1999).

However, due to its limited commercial use (Robinson *et al.* 2001), and energy-intensive production processes, the cost of commercial activated carbon remains relatively high, particularly when large quantities are needed for pollution cleanup (Rengaraj *et al.* 2002). The high costs associated with activated carbon limit its utilization. Another issue is that non-recyclable commercial materials, such as coal, are used as carbon precursors. Coal is not only costly but also contributes significantly to environmental pollution (Arulkumar *et al.* 2011). Recent years have seen the use of waste lignocellulosic substances like coconut shells, used coffee, and olive stones as alternative precursors for carbon

products. Their utilization is very promising for producing a lower-cost form of activated carbon (Noorimotlagh *et al.* 2014).

Due to the crucial role of activated carbon in various industries, increasing the lifespan of activated carbon can be highly beneficial for industry owners from a financial perspective. Enhancing adsorption involves modifying its chemical and physical properties (Domingo-García et al. 2000; Park and Jung 2002; Chen et al. 2003; Lee et al. 2005; Park et al. 2007). Among the most important methods of modification are acidic treatment (Shen et al. 2008), base treatment (Shaarani and Hameed 2011), impregnation (Yeddou et al. 2011), microwave treatment (Ania et al. 2005), ozone treatment (Zaror 1997), biological modification (Li et al. 2013), and plasma treatment (Park and Kim 2004; Bhatnagar et al. 2013). Surface plasma modification is a technique used to change the properties of materials such as polymers, carbon, and glass. It offers an efficient and cost-effective way to enhance material surfaces, making them more suitable for certain industrial and biomedical applications (Iqbal et al. 2010). Plasma contains active and highly reactive species, including electrons, ions, atoms, molecules, and radicals, which interact strongly with material surfaces (Shishoo 1996). It reacts and can have positive effects, such as increasing oxygenated functional groups, e.g. carboxylic acid (-COOH), on the surface of activated carbon (Yang et al. 2023).

Activated carbon is a valuable resource for patients with chronic kidney disease (CKD) and other diseases (Rahman *et al.* 2023), particularly in the treatment of food or drug poisoning (Jones *et al.* 1987). Its oral use can significantly reduce blood urea and phosphorus, accelerate recovery, and improve skin care products like skin scraping masks and toothpaste (Piquero-Casals *et al.* 2021). Activated carbon also finds use in extracting precious metals and refining edible oils to lighten their dark color (Mpinga *et al.* 2014).

One of the most important applications of activated carbon is in the adsorption of pollution in water environments, such as the removal of dyes and heavy metals from wastewater (Ani et al. 2020). The release of dyes as wastewater into the living environment is considered a great challenge because dyes impede light penetration into the water and cause the retardation of photosynthetic activity, which in turn prevents the entry of oxygen into the water (Regti et al. 2016; Kang et al. 2020). Dyes have a high rate of BOD and COD, and their toxicity has been proven to be harmful to aquatic species, microorganisms, and natural biological colonies (Ding et al. 2014). In addition, these substances are a main cause of mutagens and cancer in humans (Manzoor and Sharma 2020). Rhodamine B is one of the dyes that has been extensively used in the textile, printing, and paper products industries. It is also commonly used in medical labs as a biological dye (Jiang et al. 2018). rhodamine B is classified in the xanthan group; it is soluble in water, and it is a red-based cathodic dye with C<sub>28</sub>H<sub>31</sub>N<sub>2</sub>O<sub>3</sub>Cl chemical formula. At present, utilization of this coloring dye is forbidden in food, cosmetic, and hygienic industries (Mohammadi et al. 2010), because it includes four groups of N-ethyl located on either side of xanthane, which makes this compound toxic and dangerous. The most common forms of effects of this dye in humans are sexual abnormalities, digestive problems, and breathing difficulties (Rochat et al. 1978). Experimental studies have shown that it can cause various worrisome diseases in humans and animals (Jain et al. 2007; Geng et al. 2019). Dye removal methods can be divided into three physical, chemical, and biological categories, which is one of the most common methods of adsorption that is widely used (Crini 2006). Because of its simplicity in operational process design and the system's low cost, adsorption is one of the most suitable and effective techniques for removing dye from water. Furthermore, the more important aspect is that it has a high capacity of adsorbing vast scope of pollution, such as dyes from wastewater (Abd El-Monaem *et al.* 2022; Omer *et al.* 2022; Zhou *et al.* 2022).

The purpose of this study is to investigate a new source to produce activated carbon using decayed wood in comparison with sound wood, as well as a novel method that uses high-frequency air atmosphere plasma in the DBD method to remove dyed wastewater.

#### **EXPERIMENTAL**

## **Preparation of Activated Carbon**

Activated carbon was prepared according to the method mentioned in the previous study (Bidaei *et al.* 2020). Sound and decayed (affected by rainbow fungus) beech wood was collected from the forest in Khairrood, Mazandaran; the details of the wood samples are inserted in Table 1. The wood turned into powder after skinning, chopping, and milling. Then, the wood powder was sifted by the vibrating sifter with the number 60 mesh, and the smaller pieces of the number 60 mesh (piece < 250 microns) were used to prepare activated carbon. The activating agent used was zinc chloride, which is widely used for the production of activated carbon through the chemical method (Ahmadpour and Do 1997).

**Table 1.** Physicochemical Properties of Sound and Decayed Wood, as well as Characteristics of the Produced Activated Carbon

Sample	Chemical Analysis of Beech Wood Raw Material (%)	Sound Wood (Value)	Decayed Wood (Value)	
	Lignin	31	24	
	Cellulose	50	54	
	Hemicellulose	13	16	
	Extractive materials	4	3	
	Ash	2	3	
	С	46.65	46.50	
Wood	Н	4.572	5.322	
	N	0.103	0.119	
	O (by difference)	48.675	47.97	
	Yield (%)	44.1	40	
Activated carbon	Density (g/cm <sup>3</sup> )	0.716	0.382	
Activated Carbon	Iodine Number (mg/g)	1050	1145	

Modification of activated carbon using non-thermal plasma

Figure 1 shows a schematic of the DBD system for modifying the activated carbon surface. To modify the surface of activated carbon with a dielectric barrier discharge, a high-voltage power supply with a voltage of 220 V and 50 HZ at the input and maximum output of 12 kV and frequency of 20 kHz, with the square waveform observed by the oscilloscope, and a maximum electric current of 30 mA was used. The reactor used to modify activated carbon had two stainless steel square (150 mm  $\times$  150 mm  $\times$  3 mm) electrodes. The barrier was made of Pyrex and was (200 mm  $\times$  200 mm  $\times$  3 mm) with a

spacing of 12 mm between the two electrodes. Modification was performed on both samples of activated carbon through the non-thermal plasma method for 20 min at the voltage level of 10 kV.

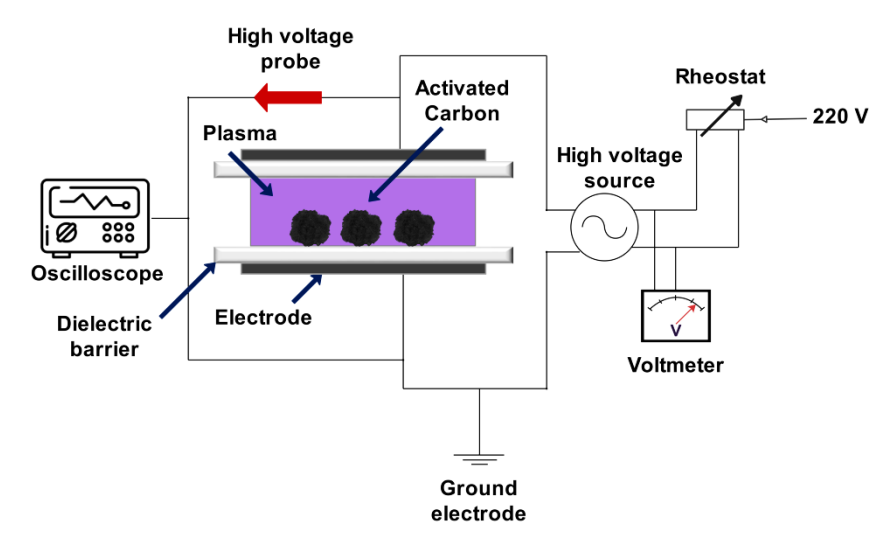


Fig. 1. Schematic design of cold plasma production and dielectric barrier discharge (DBD) reactor

#### Methods

The BET surface area, total pore volume, and pore size distribution of the activated carbon were measured using  $N_2$  adsorption (Bel Japan, Belsorp Mini II). To further analyze the surface textures and porosity evolution, scanning electron microscope (SEM) images of samples were captured before the adsorption process using an XL30 E-SEM (Philips, Eindhoven, Netherlands) instrument.

Additionally, to identify the surface groups of the activated carbons produced, they were analyzed using a Bruker Tensor 27 FTIR spectrometer. Thermal gravimetric (TG) analysis was also conducted using the NETZSCH analyzer, STA 409 PG, manufactured in Germany, to evaluate thermal stability and weight changes.

## Dye adsorption process

The rhodamine B dye adsorption process was completed using a discontinuous process. To do this, 150 ppm of soluble rhodamine dye was made. Following that, 100 mL of rhodamine B solution was mixed with 150 mg of each of the ACS, ACS-plasma, ACR, and ACR-plasma samples. This mixture was shaken at 200 rpm for 1 h at 25 °C and pH 7. After that, the mixture was filtered to isolate the solution's activated carbon. According to UV-Vis spectroscopy data, rhodamine B dye shows maximum adsorption at 555 nm. Following the preparation of standard solutions and a calibration curve, the concentration of rhodamine B dye before and after adsorption by activated carbon was measured using a UV-Vis spectrophotometer manufactured by Biochrom, and the percentage of dye removal was estimated. The dye removal (%) was calculated by the following equation (Eq. 1):

Dye removal (%)= 
$$\frac{(C_0 - C_e)}{C_0} \times 100$$
 (1)

Batch equilibrium studies

Rhodamine B dye was obtained from Sepka company, made in China, and was used as an adsorbate without undergoing any purification. All solutions were made using distilled water. The amount adsorbed  $q_e$  (mg/g) was calculated as Eq. (2),

$$q_e = \frac{(C_0 - C_e)V}{W} \tag{2}$$

where  $C_0$  and  $C_e$  (mg/L) are, respectively, the initial and equilibrium dye concentrations in the liquid phase, W is the activated carbon used (g), and V is the volume of the dye solution (L).

Study of kinetics and adsorption isotherm

Pseudo-first-order (Demirbas *et al.* 2009) and pseudo-second-order models (Al-Othman *et al.* 2012) were utilized to study RhB adsorption kinetics, as well as the adsorption mechanism and rate control processes. For this purpose, rhodamine B dye solutions of different concentrations were made. Then, 0.1 g of ACR and ACS samples were exposed to 100 mL of rhodamine B solution for 72 h. For the ACS sample, concentrations were prepared at 100, 200, 300, 400, and 500 ppm, whereas for the ACR sample, concentrations were 150, 200, 300, 400, and 500 ppm. The conditions for all the experiments were pH 7 and 25 °C. The equilibrium data were analyzed using isotherm models (Langmuir, Freundlich, and Temkin). To calculate the values of adsorption isotherms, the formulas mentioned in the literature were used (Weber and Chakravorti 1974; Haghseresht and Lu 1998; Fytianos *et al.* 2000; Tan *et al.* 2008; Erdogan 2019).

#### RESULTS AND DISCUSSION

#### Characterization of Activated Carbon

BET Analysis

Samples ACS and ACR were analyzed for nitrogen adsorption and desorption (Fig. 2). To calculate the specific surface area ( $S_{\rm BET}$ ), total pore volume ( $V_{\rm t}$ ), average pore diameter ( $D_{\rm avg}$ ) from BET, as well as to calculate the surface area ( $S_{\rm mi}$ ) and micropore volume ( $V_{\rm mi}$ ), the t-plot diagram was used. The adsorption isotherm of the samples measured according to the IUPAC classification follows the type I isotherm. According to the type of isotherm and t-plot diagram, the pores were mainly micropores and homogeneous. They are usually considered to have a cylindrical shape in this type of material.

As shown in Table 2, the BET calculation indicates that the specific surface area and total pore volume of ACS were greater than those of ACR. In addition, according to the t-plot, the area and volume of the micropores in the ACS were larger than those in the ACR, despite the mean pore diameter and iodine number being higher in the ACR. Normally, as the specific surface area and total pore volume of activated carbon increase, the capacity for pollutant adsorption also rises. However, pollutant adsorption is influenced by additional factors, including pore size, the diameter of the adsorbed molecules, and the need for low diffusion resistance (Jeirani *et al.* 2017). It is noteworthy that the specific surface area of ACS was 41% greater than that of ACR. However, the amount of dye

adsorption was much higher for the ACR sample, which may be due to the smaller pore diameter and lower density of the activated carbon derived from decayed wood.

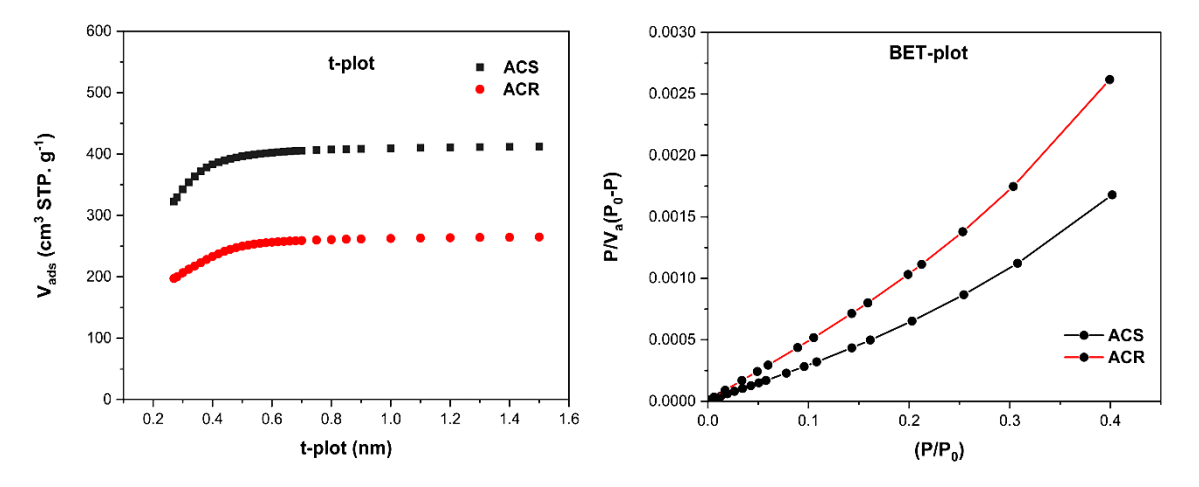


Fig. 2. N2 gas adsorption-desorption isotherms, BET, and t-plot of ACS and ACR samples

**Table 2.** Surface Area for Carbonized ACS and ACR by BET and t-plot Method Analysis

Sample		BET	t-plot		
	S <sub>BET</sub> (m <sup>2</sup> /g)	V <sub>t</sub> (cm <sup>3</sup> /g)	Davg (nm)	$S_{mi}$ (m <sup>2</sup> /g)	V <sub>mi</sub> (cm <sup>3</sup> /g)
ACS	1538	0.6493	1.6878	1836.7	0.6297
ACR	908	0.4209	1.8523	1116.1	0.4018

## SEM Analysis

Figure 3 (a, b, c, and d) shows the electron microscope image; The porous structure to adsorb pollutants in activated carbon can be clearly seen. These images reveal the structure of the primary wood material, including its pores and fibrous structure. It is clear that the activation process created a porous structure with tiny pores in the carbon surface. Holes and rough surfaces have also been observed on the surface of activated carbon produced from beech wood. This issue demonstrates that the impregnation agent affected the topographical features of the carbon surface. The image of activated carbon from sound wood (Fig. 3 (a) and (b)) and activated carbon from decayed wood (Fig. 3 (c) and (d)) make it clear that the surface of the activated carbon made from decayed wood was not smooth, and honeycomb-shaped pores can be seen. In other words, the structure of activated carbon derived from decayed wood had undergone significant destruction, leading to the complete disappearance of the precursor material's fiber structure. Therefore, it seems that the reason for this issue is the destruction of the cell wall or the destruction of the main microstructure due to fungal destruction of the precursor material. This is while the activated carbon made from sound wood maintains the shape of its fiber structure and more continuity and coherence are seen in the overall structure.

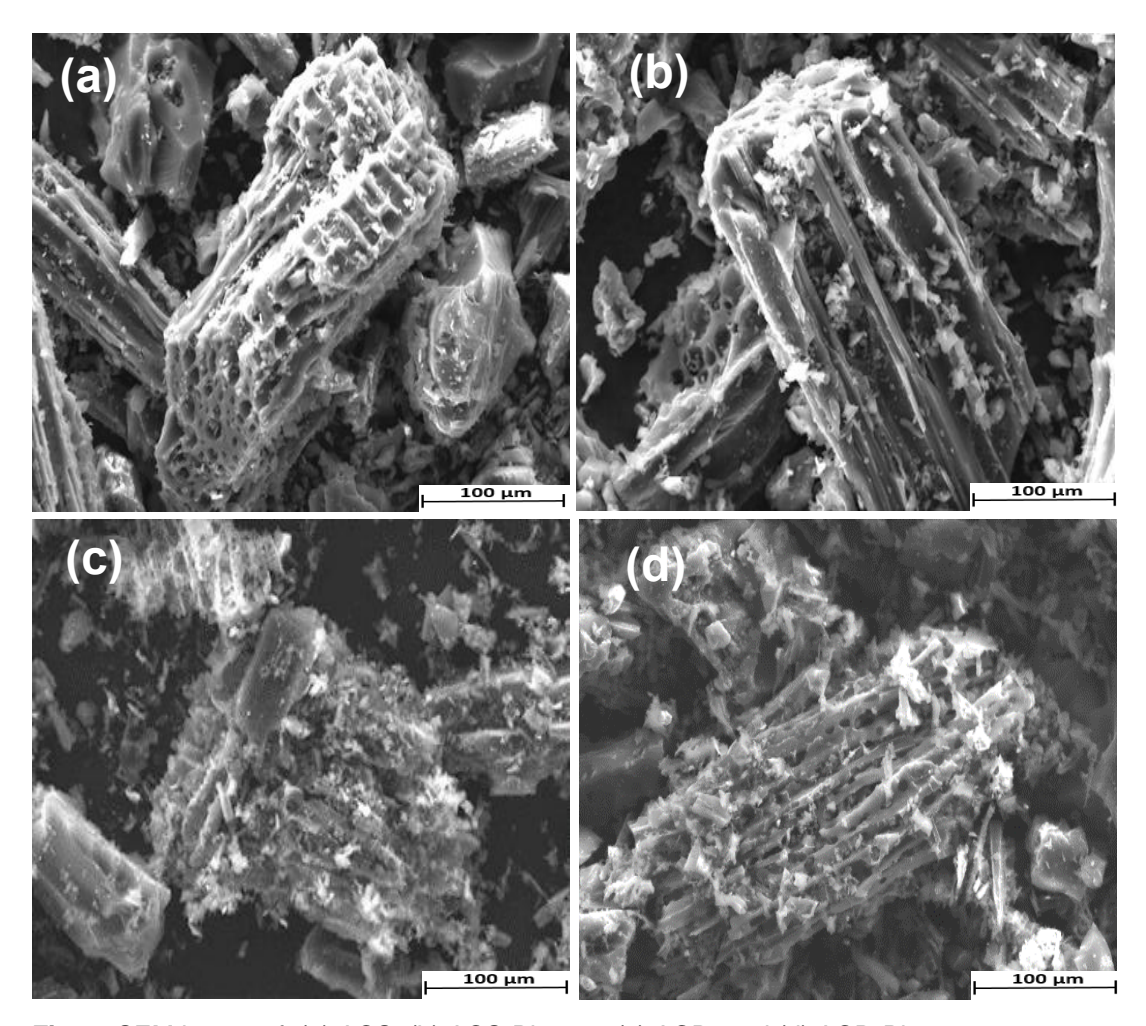


Fig. 3. SEM image of: (a) ACS, (b) ACS-Plasma, (c) ACR, and (d) ACR-Plasma

## **FTIR Analysis**

Figure 4 displays the FTIR spectra of four types of activated carbon: ACR, ACS, ACS-Plasma, and ACR-Plasma. Most of the FTIR spectra were qualitatively similar to each other, and no new peaks appeared due to modification with plasma, except that the absorbance bands in the wavenumbers of 1250, 1570, and 3440 cm<sup>-1</sup> were different in terms of the intensity of the peaks; 1250 cm<sup>-1</sup> is related to phenolic compounds, ethers, and lactonic acid, 1570 cm<sup>-1</sup> is related to the carbonyl groups C=O, and 3440 cm<sup>-1</sup> is related to the hydroxyl group. The increase of this peak shows the increase of the carboxylic acid functional group in the modified sample, which is increased by plasma modification and consistent with the results of other studies (Park and Kim 2004; Bai *et al.* 2016).

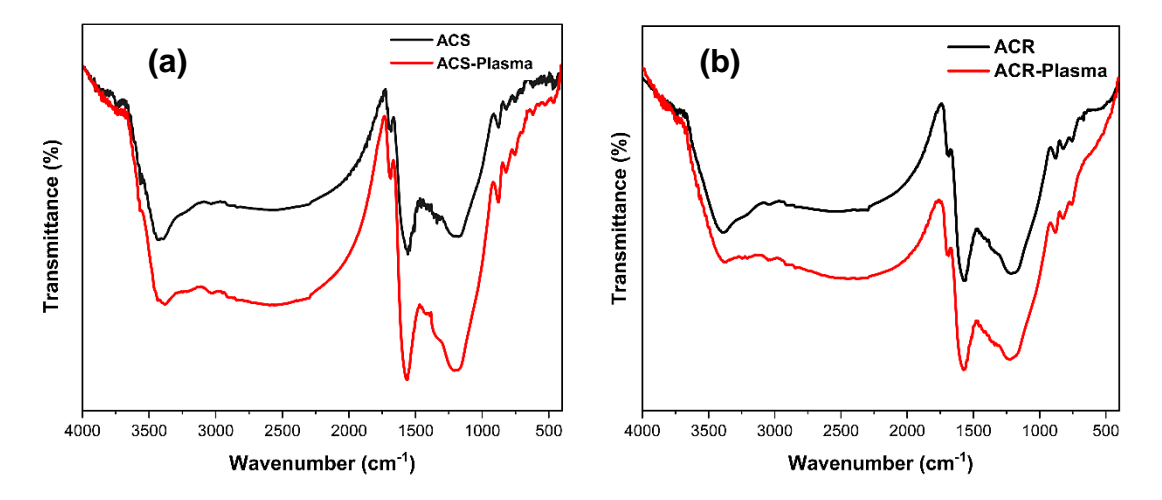


Fig. 4. FTIR of ACS and ACS-Plasma (a), ACR and ACR-Plasma (b)

## **Thermal Stability**

Figure 5 depicts the TG curve for ACS and ACR samples. Through comparing two graphs of ACS and ACR, it was discovered that at 103 °C, the weight loss in ACS was 7% and the weight loss in ACR was 10%. This temperature range releases non-flammable gases such as carbon dioxide and surface tension-limited external water, leading to weight loss. The difference in weight loss up to 103 °C between ACR and ACS can be attributed to the porous and degraded structure of ACR, which causes more water adsorption. According to the graph of the second stage, the decrease in wood mass from 103° to 390° can be attributed to the decomposition of hemicellulose, cellulose, and lignin, which partially overlaps the reactions related to their decomposition.

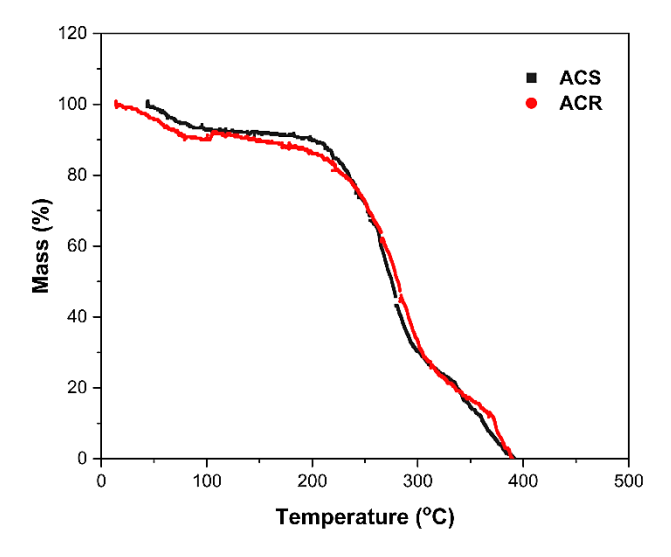


Fig. 5. TG curves of ACS and ACR samples

# Adsorption Capacities of ACS, ACR, ACS-Plasma, and ACR-Plasma

As indicated in Fig. 6, the adsorption percentage of rhodamine B dye in the activated carbon samples derived from decayed wood was considerably higher than that of

activated carbon samples from sound wood. Furthermore, surface modification using plasma enhanced adsorption by approximately 12% in the ACR sample and about 20% in the ACS sample. This finding indicates that the activated carbon derived from sound wood sample's surface treatment substantially impacted the dye adsorption efficiency more than the activated carbon derived from decayed wood sample. This disparity may be attributed to the degradation of the cell wall in the decayed wood sample or the disruption of its primary microstructure, necessitating further investigation to ascertain the underlying cause. Furthermore, it is worth noting that the activated carbon derived from decayed wood (ACR sample) exhibited greater dye adsorption than the activated carbon produced from sound wood treated with plasma (ACS-Plasma sample). This indicates the potential to use decayed wood as a useful raw material for activated carbon production.

The higher number of activated carbon microparticles per unit mass in activated carbon from decayed wood, compared to activated carbon from sound wood, could potentially explain the increased uptake of rhodamine B dye. It could also be related to the larger average diameter of micropores ( $D_{\rm avg}$ ) in activated carbon obtained from decayed wood, which warrants further investigation.

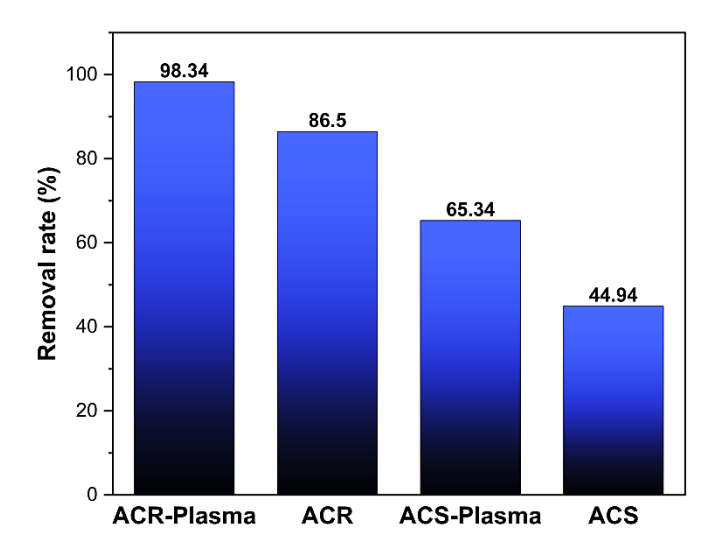


**Fig. 6.** Comparison of the percentage of adsorption of the dye rhodamine B by ACS, ACS plasma and ACR, and ACR plasma samples

Table 3 presents various published results illustrating the effect of plasma surface modification on enhancing the adsorption capacity of activated carbon. However, making direct comparisons between this study and previous research is challenging due to variations in experimental conditions and the specific compounds adsorbed by activated carbon. Unlike the typical methods of modifying activated carbon with plasma, which are conducted in the presence of specific gases, this study on surface modification of activated carbon was performed in ambient air. In this study, high voltage with a frequency of 20 kHz was used.

30

20

20

380%

20.4%

11.8%

helium and

oxygen

Air

Air

Ref	Supply	Adsorbed Material	Gas	Treatment Time (min)	Increased Adsorption (%)
(Huang <i>et</i> <i>al.</i> 2021)	8, 9, and 11 kV 10 kHz	Water vapor	Oxygen	15	100% to 400%
(Zhang <i>et al.</i> 2016)	30 kV 25 kHz	Gas-phase mercury	Oxygen	10, 20, 40	About 100%
(Che <i>et al.</i> 2013)	10 kV	SO <sub>2</sub>	Nitrogen	10, 20	Min: 11% Max: 21%
(Qu <i>et al.</i> 2013)	40 kV 200 Hz	Pentachloropheno	Oxygen Nitrogen	30	Oxygen: 0.02% Nitrogen: -0.20%
(Wu <i>et al.</i> 2012)	9 to 12 kV 50 Hz	Aniline	Oxygen	8, 16	20%
(Loo ot al	5 kV		A mixture of		

**Table 3.** The Effect of Surface Modification of Activated Carbon with Plasma on Enhancing Adsorption in Studies

# Adsorption Isotherms

(Lee et al.

2005)

ACS

plasma ACR

plasma

5 kV

10 kHz

10 kV

20 kHz

10 kV

20 kHz

The adsorption isotherm illustrates the equilibrium distribution of molecules between the liquid and solid phases. Analyzing the isotherm data and selecting the suitable model can be beneficial for design purposes (El-Geundi 1991).

Metal ions

Rhodamine B

Rhodamine B

The effect of concentration was measured for both types of activated carbon: ACS in the concentration range of 100 to 500 ppm and ACR in the range of 150 to 500 ppm, both at pH of 7.

The solutions containing some adsorbent (0.1 g) were tested after filtration. The results showed that as the concentration of rhodamine B dye increased, the percentage of dye adsorption gradually decreased because the activated carbon adsorption sites were almost completely covered at high concentrations. As the initial dye concentration increased, the amount of dye adsorbate taken up by the adsorbent per unit mass of the adsorbent also increased. This could be attributed to an increase in the number of molecules adsorbed, leading to competition for adsorption in the available sites.

The adsorption isotherm study was performed on three isotherm models, the Langmuir, Freundlich, and Temkin isotherm models, to describe the adsorption process. The goodness of fit was judged using the coefficients of determination values,  $R^2$ . The  $R^2$  value for the Langmuir isotherm was greater than 0.99 for both samples. This indicates that the findings regarding rhodamine B adsorption on activated carbon and the Langmuir isotherm are consistent. The adsorption capacity of multilayers and adsorption intensity are associated with the Freundlich isotherm, for which  $K_f$  and n are the Freundlich constants.

The value of Freundlich's constant *n* provides a measure of the desirability of adsorption; *n* values between 1 and 10 indicate optimal adsorption. Table 4 indicates that the values of *n* were 18.75 for the ACS sample and 7.83 for the ACR sample. This suggests that the adsorption for the ACS sample was unfavorable, while the adsorption for the ACR sample was favorable.

The amount of energy adsorbed in the Temkin model (B) for the adsorption of rhodamine B from an aqueous solution by both types of activated carbon (ACS and ACR) was positive, which indicates that the adsorption process was exothermic. According to Table 4, the results of adapting the dye adsorption mechanism on two adsorbents with the mentioned isotherm models are consistent with the Langmuir model.

**Table 4.** Langmuir, Freundlich, and Temkin Isotherm Model Parameters for the Adsorption of ACS and ACR Samples

Sample	Langmuir		Freundlich			Temkin			
Sample	K∟	<b>q</b> <sub>max</sub>	$R^2$	<b>K</b> <sub>f</sub>	n	R <sup>2</sup>	<b>K</b> t	В	R <sup>2</sup>
ACS	0.14	71.94	0.99	52.01	18.97	0.98	1639660	3.5	0.98
ACR	0.87	294.11	0.9999	164.78	7.83	0.72	301.81	28.70	0.76

# **Adsorption Kinetics**

Through finding the optimal contact time for the adsorbent, the equilibrium concentration can be obtained and the kinetics of the adsorption process can be understood. For this purpose, equal amounts (100 mL) of dye solution with concentrations of 100 to 500 ppm were prepared. The data were analyzed for the effect of contact with activated carbons in the amount of 0.15 g for 48 h. As mentioned earlier, pseudo-first-order and pseudo-second-order kinetic equations were used to find kinetic coefficients for adsorption of dye by activated carbon.

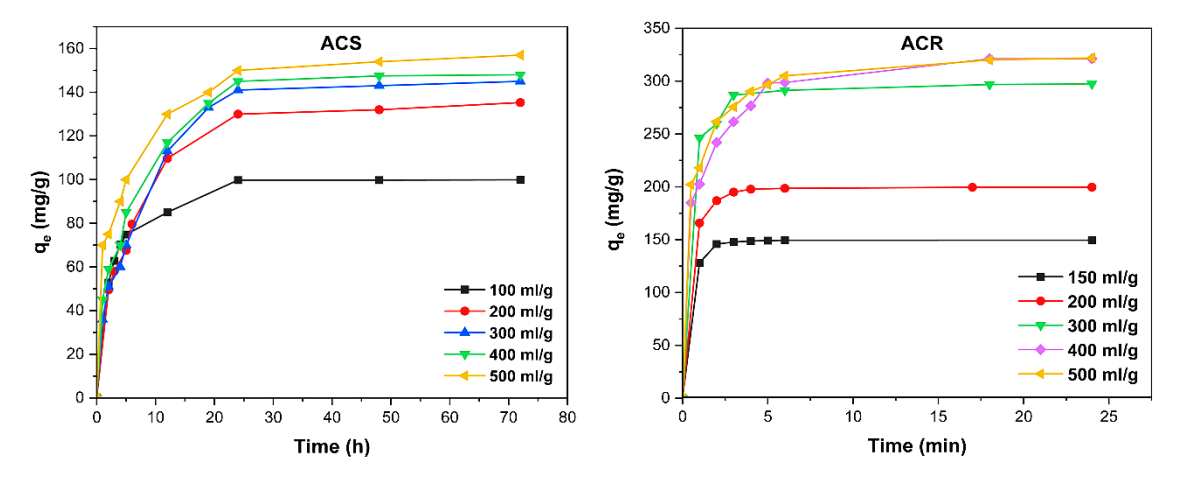


**Fig. 7.** Pseudo-second-order non-linear technique for ACS and ACR adsorption at concentrations of 100 to 500 ppm for ACS and 150 to 500 ppm for ACR

The results of rhodamine B adsorption kinetics of ACS and ACR samples are presented in Table 5, Considering the coefficient  $R^2$ , it can be deduced that both two

samples followed the second-order kinetics model. Figure 7 makes it clear that the ACR sample's major adsorption takes place in the first 2 h and the ACS sample in the first 24 h and that the adsorption values stabilize after a certain amount of time.

**Table 5.** Kinetic Parameters of Pseudo First- and Pseudo Second-order Models for the Adsorption of ACS and ACR at 25 °C

Sample	Concentration	Fi	irst-order		Second-order			
Sample	Concentration	<b>K</b> <sub>1</sub>	R <sup>2</sup>	<b>q</b> e	<b>K</b> 2	$R^2$	<b>Q</b> e	
	100 ppm	0.2778	0.9716	90.93	0.0073	0.9993	102	
	200 ppm	0.1472	0.9846	119.85	0.002	0.996	140.8	
ACS	300 ppm	0.1312	0.9887	121.049	0.0022	0.996	149.25	
	400 ppm	0.1538	0.9901	126.86	0.002	0.9986	156.25	
	500 ppm	0.1391	0.984	135.233	0.0015	0.9985	163.93	
	150 ppm*	2.164	0.9985	155.07	0.149	1	149.25	
	200 ppm	1.3882	0.9893	167.75	0.05	0.9999	200	
ASR	300 ppm	1.1796	0.838	221.18	0.021	0.9999	303	
	400 ppm	0.5751	0.9323	199.74	0.0056	0.9992	333	
	500 ppm	0.8444	0.9599	205.26	0.008	0.9996	322	

<sup>\*</sup>Because of the considerable adsorption of 100 ppm concentration in the ACR sample, 150 ppm concentration was employed to adsorb rhodamine dye

**Table 6.** Comparison of RB Maximum Adsorption Capacity ( $q_{max}$ ) of Activated Carbon in Previous Studies in the Literature

Reference	Adsorbent	Activating Agents	Adsorbent Dosage	Dye Concentration	q <sub>max</sub> (mg/g)
(Somsiripan and Sangwichien 2023)	Oil palm empty fruit bunches	Two-step activation with KOH	0.1 g	50 to 800 mg/g	982.87
(Can et al. 2023)		H <sub>3</sub> PO <sub>4</sub>	0.01 g	1000 mg/L	49.81
(Can et al. 2023)	Olive stone	KOH	0.01 g	1000 mg/L	118.26
		ZnCl <sub>2</sub>	0.01 g	1000 mg/L	256.80
(Mousavi <i>et al.</i> 2023)	Activated carbon prepared from stalk corn (namely SCBAC)	H <sub>3</sub> PO <sub>4</sub>	2.5 g	10 to 50 mg/L	5.6
(Spessato et al. 2021)	Sibipiruna activated carbon preparation by simplex-centroid mixture	KOH, K₂CO₃	25 mg	500 mg/L	646.94
(Boukerzaza et al. 2021)	Olive pomace	-	0.15 g	300 mg/L	86.20
(Xiao et al. 2020)	Activated carbon from white sugar	H <sub>2</sub> SO <sub>4</sub> , NAOH	0.08 g	50 mg/L	123.46
(Wirawan <i>et al.</i> 2020)	Spent coffee grounds (SCG)	H <sub>3</sub> PO <sub>4</sub>	0.01 g	0.5 to 12 mg/L	4.071
(Hou et al. 2019)	Bamboo shoot shell	HCI	0.04 g	300 mg/L	85.80
This study	ACS	ZnCl <sub>2</sub>	0.1 g	100-500 mg/L	71.94
This study	ACR	$ZnCl_2$	0.1 g	100-500 mg/L	294.11

Table 6 compares the maximum adsorption capacity  $(q_{\text{max}})$  of rhodamine B dye with some reported activated carbons derived from various studies.

In this study, the adsorption of rhodamine B dye was examined; however, activated carbon produced from various lignocellulosic sources has diverse applications. For instance, activated carbon prepared from *Cannabis sativum* Hemp (CSH) was utilized as an effective adsorbent for removing drug contaminants from aqueous solutions (Sajid *et al.* 2022). Similarly, the adsorption of heavy metals, dyes, and crude oil components from aquatic environments using biomass materials was investigated (Ani *et al.* 2020). The popularity of using lignocellulosic biomass is due to its low cost, wide availability, and high performance in removing various pollutants from aqueous solutions. Using decayed wood, an unused material with great abundance compared to other inexpensive sources of activated carbon production, can be an effective method for producing activated carbon.

#### CONCLUSIONS

- According to the results of the present study, decayed beech wood, as a waste material, can be regarded as a novel and promising source for producing activated carbon. It showed enhanced efficiency in adsorbing rhodamine B dye compared to activated carbon derived from sound beech wood. Beech wood, as a suitable lignocellulose material, showed excellent ability to produce activated carbon with a very high surface area. In particular, its decayed wood, which has no value for papermaking, showed superior adsorption capability.
- 2. The activated carbon sample made from decayed wood (ACR) exhibited 42% more adsorption of rhodamine B dye compared to the activated carbon sample made from sound wood (ACS).
- 3. Langmuir, Freundlich, and Temkin adsorption isotherms for ACS and ACR calculated that the adsorption of two samples follow the Langmuir and  $q_{\rm m}$  isotherms for ACS and ACR samples, respectively 71.9 and 294 mg/g, and the initial dye concentration range was 100 to 500 mg/L. The adsorption of rhodamine B from an aqueous solution follows pseudo-second-order kinetics.
- 4. One of the advantages of using low temperatures in the production of activated carbon is that it consumes less energy, which reduces production costs and contributes to lessening environmental impact. In this way, the use of decayed wood allows the use of low temperatures to produce highly adsorbent activated carbon.
- 5. In this study, plasma surface modification was applied at room temperature and in an air atmosphere. The surface modification of carbon by plasma increases surface functional groups, especially carboxylic acids, *etc.*, and thus increases the adsorption capacity of the adsorbent. Surface modification of activated carbon in the presence of air resulted in a 20% increase in rhodamine B removal for ACS and 12% for ACR.
- 6. This finding demonstrates that the surface treatment applied to the activated carbon derived from sound wood sample had a more pronounced impact on the efficiency of dye adsorption compared to the activated carbon derived from decayed wood sample.

The use of plasma in this method is important due to its simplicity, low cost, and enhanced adsorption capacity in activated carbon.

#### **ACKNOWLEDGEMENTS**

The authors are grateful to the University of Tehran (Iran) and the Air Pollution Research Center at the Iran University of Medical Sciences for their support of this research. The authors also thank Dr. Mehdi Rahmaninia for his kind consultation during the project.

## REFERENCES CITED

- Abd El-Monaem, E. M., Eltaweil, A. S., Elshishini, H. M., Hosny, M., Abou Alsoaud, M. M., Attia, N. F., El-Subruiti, G. M., and Omer, A. M. (2022). "Sustainable adsorptive removal of antibiotic residues by chitosan composites: An insight into current developments and future recommendations," *Arabian Journal of Chemistry* 15(5), article ID 103743. DOI: 10.1016/j.arabjc.2022.103743
- Ahmadpour, A., and Do, D. (1997). "The preparation of activated carbon from macadamia nutshell by chemical activation," *Carbon* 35(12), 1723-1732. DOI: 10.1016/S0008-6223(97)00127-9
- Al-Othman, Z. A., Ali, R., and Naushad, M. (2012). "Hexavalent chromium removal from aqueous medium by activated carbon prepared from peanut shell: Adsorption kinetics, equilibrium and thermodynamic studies," *Chemical Engineering Journal* 184, 238-247. DOI: 10.1016/j.cej.2012.01.048
- Ani, J. U., Akpomie, K. G., Okoro, U. C., Aneke, L. E., Onukwuli, O. D., and Ujam, O. T. (2020). "Potentials of activated carbon produced from biomass materials for sequestration of dyes, heavy metals, and crude oil components from aqueous environment," *Applied Water Science* 10(2), article 69. DOI: 10.1007/s13201-020-1149-8
- Ania, C. O., Parra, J. B., Menéndez, J. A., and Pis, J. J. (2005). "Effect of microwave and conventional regeneration on the microporous and mesoporous network and on the adsorptive capacity of activated carbons," *Microporous and Mesoporous Materials* 85(1), 7-15. DOI: 10.1016/j.micromeso.2005.06.013
- Arulkumar, M., Sathishkumar, P., and Palvannan, T. (2011). "Optimization of Orange G dye adsorption by activated carbon of *Thespesia populnea* pods using response surface methodology," *Journal of Hazardous Materials* 186(1), 827-834. DOI: 10.1016/j.jhazmat.2010.11.067
- Bai, B. C., Lee, H.-U., Lee, C. W., Lee, Y.-S., and Im, J. S. (2016). "N<sub>2</sub> plasma treatment on activated carbon fibers for toxic gas removal: Mechanism study by electrochemical investigation," *Chemical Engineering Journal* 306, 260-268. DOI: 10.1016/j.cej.2016.07.046
- Bhatnagar, A., Hogland, W., Marques, M., and Sillanpää, M. (2013). "An overview of the modification methods of activated carbon for its water treatment applications," *Chemical Engineering Journal* 219, 499-511. DOI: 10.1016/j.cej.2012.12.038

- Bidaei, M. R., Yarahmadi, R., and Azadfallah, M. (2020). "Effect of surface modification of activated carbon by cold plasma on the adsorption capacity of Rhodamine B," *Iran Occupational Health* 17, article 15.
- Blasi, A., Verardi, A., Lopresto, C. G., Siciliano, S., and Sangiorgio, P. (2023). "Lignocellulosic agricultural waste valorization to obtain valuable products: An overview," *Recycling* 8(4), article 61. DOI: 10.3390/recycling8040061
- Boukerzaza, I.-M., Boulhouchet, B., Kebabi, B., and Mennour, A. (2021). "Adsorption of Rhodamine b onto olive pomace: Isotherms, kinetics and infrared studies," *Environmental Engineering & Management Journal (EEMJ)* 20(12), 1963-1971. DOI: 10.30638/eemj.2021.183
- Can, M., Ozcan, D. O., and Bikem, O. (2023). "Extremely efficient adsorption of Rhodamine B dye from aqueous solutions onto modified olive stone activated carbon: Modelling and optimization studies," Research Square, (Preprint). DOI: 10.21203/rs.3.rs-3469134/v1
- Che, Y., Zhou, J., and Wang, Z. (2013). "Plasma modification of activated carbon fibers for adsorption of SO<sub>2</sub>," *Plasma Science and Technology* 15(10), 1047-1052. DOI: 10.1088/1009-0630/15/10/16
- Chen, J. P., Wu, S., and Chong, K.-H. (2003). "Surface modification of a granular activated carbon by citric acid for enhancement of copper adsorption," *Carbon* 41(10), 1979-1986. DOI: 10.1016/S0008-6223(03)00197-0
- Crini, G. (2006). "Non-conventional low-cost adsorbents for dye removal: A review," *Bioresource Technology* 97(9), 1061-1085. DOI: 10.1016/j.biortech.2005.05.001
- Demirbas, E., Dizge, N., Sulak, M. T., and Kobya, M. (2009). "Adsorption kinetics and equilibrium of copper from aqueous solutions using hazelnut shell activated carbon," *Chemical Engineering Journal* 148(2), 480-487. DOI: 10.1016/j.cej.2008.09.027
- Ding, L., Zou, B., Gao, W., Liu, Q., Wang, Z., Guo, Y., Wang, X., and Liu, Y. (2014). "Adsorption of Rhodamine-B from aqueous solution using treated rice husk-based activated carbon," *Colloids and Surfaces A: Physicochemical and Engineering Aspects* 446, 1-7. DOI: 10.1016/j.colsurfa.2014.01.030
- Domingo-García, M., López-Garzón, F. J., and Pérez-Mendoza, M. (2000). "Effect of some oxidation treatments on the textural characteristics and surface chemical nature of an activated carbon," *Journal of Colloid Interface Science* 222(2), 233-240. DOI: 10.1006/jcis.1999.6619
- El-Geundi, M. S. (1991). "Homogeneous surface diffusion model for the adsorption of basic dyestuffs onto natural clay in batch adsorbers," *Adsorption Science & Technology* 8, 217-225. DOI: 10.1177/0263617491008004
- Erdogan, F. O. (2019). "Freundlich, Langmuir, Temkin, DR and Harkins-Jura isotherm studies on the adsorption of CO<sub>2</sub> on various porous adsorbents," *International Journal of Chemical Reactor Engineering* 17(5), article ID 20180134. DOI: 10.1515/ijcre-2018-0134
- Fytianos, K., Voudrias, E., and Kokkalis, E. (2000). "Sorption–desorption behaviour of 2,4-dichlorophenol by marine sediments," *Chemosphere* 40(1), 3-6. DOI: 10.1016/S0045-6535(99)00214-3
- Geng, J., Gu, F., and Chang, J. (2019). "Fabrication of magnetic lignosulfonate using ultrasonic-assisted in situ synthesis for efficient removal of Cr(VI) and Rhodamine B

- from wastewater," *Journal of Hazardous Materials* 375, 174-181. DOI: 10.1016/j.ihazmat.2019.04.086
- Haghseresht, F., and Lu, G. Q. (1998). "Adsorption characteristics of phenolic compounds onto coal-reject-derived adsorbents," *Energy & Fuels* 12(6), 1100-1107. DOI: 10.1021/ef9801165
- Hassan, M. F., Sabri, M. A., Fazal, H., Hafeez, A., Shezad, N., and Hussain, M. (2020). "Recent trends in activated carbon fibers production from various precursors and applications—a comparative review," *Journal of Analytical and Applied Pyrolysis* 145, article ID 104715. DOI: 10.1016/j.jaap.2019.104715
- Hou, Y., Huang, G., Li, J., Yang, Q., Huang, S., and Cai, J. (2019). "Hydrothermal conversion of bamboo shoot shell to biochar: Preliminary studies of adsorption equilibrium and kinetics for rhodamine B removal," *Journal of Analytical and Applied Pyrolysis* 143, Article ID 104694. DOI: 10.1016/j.jaap.2019.104694
- Huang, Y., Yu, Q., Li, M., Jin, S., Fan, J., Zhao, L., and Yao, Z. (2021). "Surface modification of activated carbon fiber by low-temperature oxygen plasma: Textural property, surface chemistry, and the effect of water vapor adsorption," *Chemical Engineering Journal* 418, Article ID 129474. DOI: 10.1016/j.cej.2021.129474
- Iqbal, H. M. S., Bhowmik, S., and Benedictus, R. (2010). "Surface modification of high performance polymers by atmospheric pressure plasma and failure mechanism of adhesive bonded joints," *International Journal of Adhesion and Adhesives* 30(6), 418-424. DOI: 10.1016/j.ijadhadh.2010.02.007
- Jain, R., Mathur, M., Sikarwar, S., and Mittal, A. (2007). "Removal of the hazardous dye rhodamine B through photocatalytic and adsorption treatments," *Journal of Environmental Management* 85(4), 956-964. DOI: 10.1016/j.jenvman.2006.11.002
- Jeirani, Z., Niu, C. H., and Soltan, J. (2017). "Adsorption of emerging pollutants on activated carbon," *Reviews in Chemical Engineering* 33(5), 491-522. DOI: 10.1515/revce-2016-0027
- Jiang, L., Zhang, Y., Zhou, M., Liang, L., and Li, K. (2018). "Oxidation of Rhodamine B by persulfate activated with porous carbon aerogel through a non-radical mechanism," *Journal of Hazardous Materials* 358, 53-61. DOI: 10.1016/j.jhazmat.2018.06.048
- Jjagwe, J., Olupot, P. W., Menya, E., and Kalibbala, H. M. (2021). "Synthesis and application of granular activated carbon from biomass waste materials for water treatment: A review," *Journal of Bioresources and Bioproducts* 6(4), 292-322. DOI: 10.1016/j.jobab.2021.03.003
- Jones, J., McMullen, M. J., Dougherty, J., and Cannon, L. (1987). "Repetitive doses of activated charcoal in the treatment of poisoning," *The American Journal of Emergency Medicine* 5(4), 305-311. DOI: 10.1016/0735-6757(87)90358-5
- Kang, S., Qin, L., Zhao, Y., Wang, W., Zhang, T., Yang, L., Rao, F., and Song, S. (2020). "Enhanced removal of methyl orange on exfoliated montmorillonite/chitosan gel in presence of methylene blue," *Chemosphere* 238, article ID 124693. DOI: 10.1016/j.chemosphere.2019.124693
- Karim, M., Daryaei, M. G., Torkaman, J., Oladi, R., Ghanbary, M. A. T., and Bari, E. (2016). "In vivo investigation of chemical alteration in oak wood decayed by *Pleurotus ostreatus*," International Biodeterioration & Biodegradation 108, 127-132. DOI: 10.1016/j.ibiod.2015.12.012

- Lee, D., Hong, S. H., Paek, K.-H., and Ju, W.-T. (2005). "Adsorbability enhancement of activated carbon by dielectric barrier discharge plasma treatment," *Surface and Coatings Technology* 200(7), 2277-2282. DOI: 10.1016/j.surfcoat.2004.11.027
- Li, B. J., Hu, J., Huang, L. Y., Lv, Y., Zuo, J., Zhang, W., Ying, W. C., and Matsumoto, M. R. (2013). "Removal of MTBE in biological activated carbon adsorbers," *Environmental Progress & Sustainable Energy* 32(2), 239-248. DOI: 10.1002/ep.11614
- Manzoor, J., and Sharma, M. (2020). "Impact of textile dyes on human health and environment," in: *Impact of Textile Dyes on Public Health and the Environment*, IGI Global, Hershey, PA, USA, pp. 162-169. DOI: 10.4018/978-1-7998-0311-9
- Mohammadi, M., Hassani, A. J., Mohamed, A. R., and Najafpour, G. D. (2010). "Removal of Rhodamine B from aqueous solution using palm shell-based activated carbon: Adsorption and kinetic studies," *Journal of Chemical & Engineering Data* 55(12), 5777-5785. DOI: 10.1021/je100730a
- Mousavi, S. A., Kamarehie, B., Almasi, A., Darvishmotevalli, M., Salari, M., Moradnia, M., Azimi, F., Ghaderpoori, M., Neyazi, Z., and Karami, M. A. (2023). "Removal of Rhodamine B from aqueous solution by stalk corn activated carbon: Adsorption and kinetic study," *Biomass Conversion and Biorefinery* 13(9), 7927-7936. DOI: 10.1007/s13399-021-01628-1
- Mpinga, C. N., Bradshaw, S. M., Akdogan, G., Snyders, C. A., and Eksteen, J. J. (2014). "The extraction of Pt, Pd and Au from an alkaline cyanide simulated heap leachate by granular activated carbon," *Minerals Engineering* 55, 11-17. DOI: 10.1016/j.mineng.2013.09.001
- Müller, J., and Bütler, R. (2010). "A review of habitat thresholds for dead wood: A baseline for management recommendations in European forests," *European Journal of Forest Research* 129(6), 981-992. DOI: 10.1007/s10342-010-0400-5
- Noorimotlagh, Z., Darvishi Cheshmeh Soltani, R., Khataee, A. R., Shahriyar, S., and Nourmoradi, H. (2014). "Adsorption of a textile dye in aqueous phase using mesoporous activated carbon prepared from Iranian milk vetch," *Journal of the Taiwan Institute of Chemical Engineers* 45(4), 1783-1791. DOI: 10.1016/j.jtice.2014.02.017
- Omer, A. M., Dey, R., Eltaweil, A. S., Abd El-Monaem, E. M., and Ziora, Z. M. (2022). "Insights into recent advances of chitosan-based adsorbents for sustainable removal of heavy metals and anions," *Arabian Journal of Chemistry* 15(2), Article ID 103543. DOI: 10.1016/j.arabjc.2021.103543
- Park, S.-J., and Jung, W.-Y. (2002). "Preparation and structural characterization of activated carbons based on polymeric resin," *Journal of Colloid and Interface Science* 250(1), 196-200. DOI: 10.1006/jcis.2002.8337
- Park, S.-J., and Kim, B.-J. (2004). "Influence of oxygen plasma treatment on hydrogen chloride removal of activated carbon fibers," *Journal of Colloid and Interface Science* 275(2), 590-595. DOI: 10.1016/j.jcis.2004.03.011
- Park, B. K., Jeong, S., Kim, D., Moon, J., Lim, S., and Kim, J. S. (2007). "Synthesis and size control of monodisperse copper nanoparticles by polyol method," *Journal of Colloid Interface Science* 311(2), 417-424. DOI: 10.1016/j.jcis.2007.03.039
- Periyasamy, S., Karthik, V., Senthil Kumar, P., Isabel, J. B., Temesgen, T., Hunegnaw, B. M., Melese, B. B., Mohamed, B. A., and Vo, D.-V. N. (2022). "Chemical, physical

- and biological methods to convert lignocellulosic waste into value-added products. A review," *Environmental Chemistry Letters* 20(2), 1129-1152. DOI: 10.1007/s10311-021-01374-w
- Piquero-Casals, J., Morgado-Carrasco, D., Granger, C., Trullàs, C., Jesús-Silva, A., and Krutmann, J. (2021). "Urea in dermatology: A review of its emollient, moisturizing, keratolytic, skin barrier enhancing and antimicrobial properties," *Dermatol Ther* (*Heidelb*) 11(6), 1905-1915. DOI: 10.1007/s13555-021-00611-y
- Qu, G.-Z., Li, J., Liang, D.-L., Huang, D.-L., Qu, D., and Huang, Y.-M. (2013). "Surface modification of a granular activated carbon by dielectric barrier discharge plasma and its effects on pentachlorophenol adsorption," *Journal of Electrostatics* 71(4), 689-694. DOI: 10.1016/j.elstat.2013.03.013
- Rahman, W. K., Rabea, I. S., and Meizel, M. M. (2023). "Protective effect of activated charcoal against progression of chronic kidney disease: A randomized clinical study," *J Med Life* 16(9), 1310-1315. DOI: 10.25122/jml-2023-0128
- Regti, A., Ayouchia, H. B. E., Laamari, M. R., Stiriba, S. E., Anane, H., and Haddad, M. E. (2016). "Experimental and theoretical study using DFT method for the competitive adsorption of two cationic dyes from wastewaters," *Applied Surface Science* 390, 311-319. DOI: 10.1016/j.apsusc.2016.08.059
- Rengaraj, S., Moon, S.-H., Sivabalan, R., Arabindoo, B., and Murugesan, V. (2002). "Removal of phenol from aqueous solution and resin manufacturing industry wastewater using an agricultural waste: Rubber seed coat," *Journal of Hazardous Materials* 89(2), 185-196. DOI: 10.1016/S0304-3894(01)00308-9
- Robinson, T., McMullan, G., Marchant, R., and Nigam, P. (2001). "Remediation of dyes in textile effluent: A critical review on current treatment technologies with a proposed alternative," *Bioresource Technology* 77(3), 247-255. DOI: 10.1016/S0960-8524(00)00080-8
- Rochat, J., Demenge, P., and Rerat, J. (1978). "Toxicologic study of a fluorescent tracer: Rhodamine B," *Toxicological European Research* 1(1), 23-26.
- Sajid, M., Bari, S., Rehman, M. S. U., Ashfaq, M., Guoliang, Y., and Mustafa, G. (2022). "Adsorption characteristics of paracetamol removal onto activated carbon prepared from *Cannabis sativum* Hemp," *Alexandria Engineering Journal* 61(9), 7203-7212. DOI: 10.1016/j.aej.2021.12.060
- Schwarze, F. W. M. R. (2007). "Wood decay under the microscope," *Fungal Biology Reviews* 21(4), 133-170. DOI: 10.1016/j.fbr.2007.09.001
- Shaarani, F. W., and Hameed, B. H. (2011). "Ammonia-modified activated carbon for the adsorption of 2,4-dichlorophenol," *Chemical Engineering Journal* 169(1), 180-185. DOI: 10.1016/j.cej.2011.03.002
- Shen, W., Li, Z., and Liu, Y. (2008). "Surface chemical functional groups modification of porous carbon," *Recent Patents on Chemical Engineering* 1(1), 27-40. DOI: 10.2174/1874478810801010027
- Shishoo, R. (1996). "Plasma treatment—Industrial applications and its impact on the C&L industry," *Journal of Coated Fabrics* 26(1), 26-35. DOI: 10.1177/152808379602600104
- Somsiripan, T., and Sangwichien, C. (2023). "Enhancement of adsorption capacity of Methylene blue, Malachite green, and Rhodamine B onto KOH activated carbon

- derived from decayed wood erived from oil palm empty fruit bunches," *Arabian Journal of Chemistry* 16(12), article ID 105270. DOI: 10.1016/j.arabjc.2023.105270
- Spessato, L., Duarte, V. A., Viero, P., Zanella, H., Fonseca, J. M., Arroyo, P. A., and Almeida, V. C. (2021). "Optimization of Sibipiruna activated carbon preparation by simplex-centroid mixture design for simultaneous adsorption of Rhodamine B and metformin," *Journal of Hazardous Materials* 411, article ID 125166. DOI: 10.1016/j.jhazmat.2021.125166
- Sung, J.-H., Back, S.-K., Lee, E.-S., Jang, H.-N., Seo, Y.-C., Kang, Y.-S., and Lee, M.-H. (2019). "Application of powdered activated carbon coating to fabrics in a hybrid filter to enhance mercury removal," *Journal of Environmental Sciences* 80, 58-65. DOI: 10.1016/j.jes.2018.08.004
- Świątkowski, A. (1999). "Industrial carbon adsorbents," *Studies in Surface Science and Catalysis* 120, 69-94. DOI: 10.1016/S0167-2991(99)80549-7
- Tan, I. A. W., Ahmad, A. L., and Hameed, B. H. (2008). "Adsorption of basic dye on high-surface-area activated carbon prepared from coconut husk: Equilibrium, kinetic and thermodynamic studies," *Journal of Hazardous Materials* 154(1), 337-346. DOI: 10.1016/j.jhazmat.2007.10.031
- Weber, T. W., and Chakravorti, R. K. (1974). "Pore and solid diffusion models for fixed-bed adsorbers," *AIChE Journal* 20(2), 228-238. DOI: 10.1002/aic.690200204
- Wee, J.-H., Bae, Y., Ahn, H., Choi, Y. O., Jeong, E., and Yeo, S. Y. (2022). "Fibrous and granular activated carbon mixed media for effective gas removal as a cabin air filter," *Carbon Letters* 32(4), 1111-1118. DOI: 10.1007/s42823-022-00345-7
- Wirawan, T., Koesnarpadi, S., and Widodo, N. T. (2020). "Study of Rhodamine B adsorption onto activated carbon from spent coffee grounds," *AIP Conference Proceedings* 2237(1), article ID 020007. DOI: 10.1063/5.0005610
- Wu, G.-Q., Zhang, X., Hui, H., Yan, J., Zhang, Q.-S., Wan, J.-L., and Dai, Y. (2012). "Adsorptive removal of aniline from aqueous solution by oxygen plasma irradiated bamboo based activated carbon," *Chemical Engineering Journal* 185-186, 201-210. DOI: 10.1016/j.cej.2012.01.084
- Xiao, W., Garba, Z. N., Sun, S., Lawan, I., Wang, L., Lin, M., and Yuan, Z. (2020). "Preparation and evaluation of an effective activated carbon from white sugar for the adsorption of rhodamine B dye," *Journal of Cleaner Production* 253, article ID 119989. DOI: 10.1016/j.jclepro.2020.119989
- Yang, S. Y., Bai, B. C., and Kim, Y. R. (2023). "Effective surface structure changes and characteristics of activated carbon with the simple introduction of oxygen functional groups by using radiation energy," *Surfaces* 7(1), 12-25. DOI: 10.3390/surfaces7010002
- Yeddou, A. R., Chergui, S., Chergui, A., Halet, F., Hamza, A., Nadjemi, B., Ould-Dris, A., and Belkouch, J. (2011). "Removal of cyanide in aqueous solution by oxidation with hydrogen peroxide in presence of copper-impregnated activated carbon," *Minerals Engineering* 24(8), 788-793. DOI: 10.1016/j.mineng.2011.02.012
- Zaror, C. A. (1997). "Enhanced oxidation of toxic effluents using simultaneous ozonation and activated carbon treatment," *Journal of Chemical Technology & Biotechnology* 70(1), 21-28. DOI: 10.1002/(SICI)1097-4660(199709)70:1<21::AID-JCTB706>3.0.CO;2-3

- Zhang, J., Duan, Y., Zhou, Q., Zhu, C., She, M., and Ding, W. (2016). "Adsorptive removal of gas-phase mercury by oxygen non-thermal plasma modified activated carbon," *Chemical Engineering Journal* 294, 281-289. DOI: 10.1016/j.cej.2016.02.002
- Zhou, Q., Wu, Y., Chen, H., Zhu, G., Zhang, Y., Liang, D., Chen, G., and Tang, S. (2022). "Preparation of *Quercus mongolica* leaf-derived porous carbon with a large specific surface area for highly effective removal of dye and antibiotic from water," *Arabian Journal of Chemistry* 15(9), article ID 104031. DOI: 10.1016/j.arabjc.2022.104031

Article submitted: August 08, 2024; Peer review completed: September 14, 2024; Revised version received: October 5, 2024; Accepted: October 11, 2024; Published: October 27, 2024.

DOI: 10.15376/biores.19.4.9510-9530